

Facile metal transfer method for fabricating unconventional metamaterial devices

Mei Zhu and Chengkuo Lee*

Department of Electrical and Computer Engineering, National University of Singapore, 4 Engineering Drive 3, Singapore 117576, Singapore

*elelc@nus.edu.sg

Abstract: We report a facile metal transfer method to create metal patterns on polydimethylsiloxane (PDMS) surface. The metals were first patterned on polyethylene terephthalate (PET) substrate, and then transferred to PDMS simply by oxygen plasma treatment. The transfer was enabled by weakened metal-PET adhesion due to undercut and charge repulsion. In this way, we got rid of adhesion layers and sacrificial layers that were required by conventional methods. Ours is a fast and convenient method as it takes place at room temperature with just a gentle contact of PET and PDMS. The resolution of this method was found to be in sub-micron range and the morphologies of different transferred patterns were characterized. With such a method, we successfully fabricated some unconventional metamaterial devices, including a double-sided broadband THz filter with a stop band bandwidth of 1.4 THz, and devices on paper, fabric, leaf and non-planar surfaces.

©2015 Optical Society of America

OCIS codes: (220.4610) Optical fabrication; (160.3918) Metamaterials; (230.7408) Wavelength filtering devices.

References and links

1. S. C. B. Mannsfeld, B. C.-K. Tee, R. M. Stoltenberg, C. V. H.-H. Chen, S. Barman, B. V. O. Muir, A. N. Sokolov, C. Reese, and Z. Bao, "Highly sensitive flexible pressure sensors with microstructured rubber dielectric layers," *Nat. Mater.* **9**(10), 859–864 (2010).
2. J. C. Lötters, W. Olthuis, P. H. Veltink, and P. Bergveld, "The mechanical properties of the rubber elastic polymer polydimethylsiloxane for sensor applications," *J. Micromech. Microeng.* **7**(3), 145–147 (1997).
3. M. Zhu, L. Zhou, B. Li, M. K. Dawood, G. Wan, C. Q. Lai, H. Cheng, K. C. Leong, R. Rajagopalan, H. P. Too, and W. K. Choi, "Creation of nanostructures by interference lithography for modulation of cell behavior," *Nanoscale* **3**(7), 2723–2729 (2011).
4. T. Sekitani, H. Nakajima, H. Maeda, T. Fukushima, T. Aida, K. Hata, and T. Someya, "Stretchable active-matrix organic light-emitting diode display using printable elastic conductors," *Nat. Mater.* **8**(6), 494–499 (2009).
5. Z. Wang, J. Yuan, J. Zhang, R. Xing, D. Yan, and Y. Han, "Metal transfer printing and its application in organic field-effect transistor fabrication," *Adv. Mater.* **15**(12), 1009–1012 (2003).
6. J. G. Kim, N. Takama, B. J. Kim, and H. Fujita, "Optical-softlithographic technology for patterning on curved surfaces," *J. Micromech. Microeng.* **19**(5), 055017 (2009).
7. J. B. Pendry, A. Holden, D. Robbins, and W. Stewart, "Magnetism from conductors and enhanced nonlinear phenomena," *IEEE Trans. Microw. Theory Tech.* **47**(11), 2075–2084 (1999).
8. R. A. Shelby, D. R. Smith, and S. Schultz, "Experimental verification of a negative index of refraction," *Science* **292**(5514), 77–79 (2001).
9. T. J. Yen, W. J. Padilla, N. Fang, D. C. Vier, D. R. Smith, J. B. Pendry, D. N. Basov, and X. Zhang, "Terahertz magnetic response from artificial materials," *Science* **303**(5663), 1494–1496 (2004).
10. C. M. Soukoulis, S. Linden, and M. Wegener, "Physics. Negative refractive index at optical wavelengths," *Science* **315**(5808), 47–49 (2007).
11. Y. S. Lin and C. Lee, "Tuning characteristics of mirrorlike T-shape terahertz metamaterial using out-of-plane actuated cantilevers," *Appl. Phys. Lett.* **104**(25), 251914 (2014).
12. F. Ma, Y. S. Lin, X. Zhang, and C. Lee, "Tunable multiband terahertz metamaterials using a reconfigurable electric split-ring resonator array," *Light. Science and Applications* **3**(5), e171 (2014).
13. P. Pitchappa, C. P. Ho, Y. Lin, P. Kropelnicki, C. Huang, N. Singh, and C. Lee, "Micro-electro-mechanically tunable metamaterial with enhanced electro-optic performance," *Appl. Phys. Lett.* **104**(15), 151104 (2014).
14. I. M. Pryce, K. Aydin, Y. A. Kelaita, R. M. Briggs, and H. A. Atwater, "Highly strained compliant optical metamaterials with large frequency tunability," *Nano Lett.* **10**(10), 4222–4227 (2010).

15. S. Aksu, M. Huang, A. Artar, A. A. Yanik, S. Selvarasah, M. R. Dokmeci, and H. Altug, "Flexible plasmonics on unconventional and nonplanar substrates," *Adv. Mater.* **23**(38), 4422–4430 (2011).
16. J. Li, C. M. Shah, W. Withayachumnankul, B. S.-Y. Ung, A. Mitchell, S. Sriram, M. Bhaskaran, S. Chang, and D. Abbott, "Mechanically tunable terahertz metamaterials," *Appl. Phys. Lett.* **102**(12), 121101 (2013).
17. J. Li, C. M. Shah, W. Withayachumnankul, B. S.-Y. Ung, A. Mitchell, S. Sriram, M. Bhaskaran, S. Chang, and D. Abbott, "Flexible terahertz metamaterials for dual-axis strain sensing," *Opt. Lett.* **38**(12), 2104–2106 (2013).
18. C. Zaichun, M. Rahmani, G. Yandong, C. T. Chong, and H. Minghui, "Realization of Variable Three-Dimensional Terahertz Metamaterial Tubes for Passive Resonance Tunability," *Adv. Mater.* **24**(23), OP143–OP147 (2012).
19. R. Alaei, C. Menzel, C. Rockstuhl, and F. Lederer, "Perfect absorbers on curved surfaces and their potential applications," *Opt. Express* **20**(16), 18370–18376 (2012).
20. R. Yahiaoui, J. P. Guillet, F. de Miollis, and P. Mounaix, "Ultra-flexible multiband terahertz metamaterial absorber for conformal geometry applications," *Opt. Lett.* **38**(23), 4988–4990 (2013).
21. I. E. Khodasevych, C. M. Shah, S. Sriram, M. Bhaskaran, W. Withayachumnankul, B. S. Y. Ung, H. Lin, W. S. T. Rowe, D. Abbott, and A. Mitchell, "Elastomeric silicone substrates for terahertz fishnet metamaterials," *Appl. Phys. Lett.* **100**(6), 061101 (2012).
22. H. Schmid, H. Wolf, R. Allenspach, H. Riel, S. Karg, B. Michel, and E. Delamarche, "Preparation of metallic films on elastomeric stamps and their application for contact processing and contact printing," *Adv. Funct. Mater.* **13**(2), 145–153 (2003).
23. J. W. Kim, K. Y. Yang, S. H. Hong, and H. Lee, "Formation of Au nano-patterns on various substrates using simplified nano-transfer printing method," *Appl. Surf. Sci.* **254**(17), 5607–5611 (2008).
24. T. Kim, A. Carlson, J. Ahn, S. M. Won, S. Wang, Y. Huang, and J. A. Rogers, "Kinetically controlled, adhesiveless transfer printing using microstructured stamps," *Appl. Phys. Lett.* **94**(11), 113502 (2009).
25. Y. L. Loo, R. L. Willett, K. W. Baldwin, and J. A. Rogers, "Additive, nanoscale patterning of metal films with a stamp and a surface chemistry mediated transfer process: Applications in plastic electronics," *Appl. Phys. Lett.* **81**(3), 562–564 (2002).
26. I. Byun, A. W. Coleman, and B. Kim, "Transfer of thin Au films to polydimethylsiloxane (PDMS) with reliable bonding using (3-mercaptopropyl)trimethoxysilane (MPTMS) as a molecular adhesive," *J. Micromech. Microeng.* **23**(8), 085016 (2013).
27. K. S. Lim, W. J. Chang, Y. M. Koo, and R. Bashir, "Reliable fabrication method of transferable micron scale metal pattern for poly(dimethylsiloxane) metallization," *Lab Chip* **6**(4), 578–580 (2006).
28. B. Li, X. Liu, M. Zhu, Z. Wang, A. O. Adeyeye, and W. K. Choi, "Synthesis and Characterization of Cobalt/Palladium Multilayer Film and Nanodiscs on Polyethylene Terephthalate Substrate," *J. Nanosci. Nanotechnol.* **15**(6), 4332–4338 (2015).
29. M. Zhu, B. Li, and W. K. Choi, "Fabrication of Nanostructures on Polyethylene Terephthalate Substrate by Interference Lithography and Plasma Etching," *J. Nanosci. Nanotechnol.* **13**(8), 5474–5480 (2013).
30. D. Kim, Y. Kim, J. Wu, Z. Liu, J. Song, H. Kim, Y. Y. Huang, K. Hwang, and J. A. Rogers, "Ultrathin Silicon Circuits With Strain-Isolation Layers and Mesh Layouts for High-Performance Electronics on Fabric, Vinyl, Leather, and Paper," *Adv. Mater.* **21**(36), 3703–3707 (2009).
31. O. Graudejus, P. Görrn, and S. Wagner, "Controlling the morphology of gold films on poly(dimethylsiloxane)," *ACS Appl. Mater. Interfaces* **2**(7), 1927–1933 (2010).
32. S. Linden, C. Enkrich, M. Wegener, J. Zhou, T. Koschny, and C. M. Soukoulis, "Magnetic response of metamaterials at 100 terahertz," *Science* **306**(5700), 1351–1353 (2004).
33. M. Zhu, Department of Electrical and Computer Engineering, National University of Singapore, 4 Engineering Drive 3, Singapore 117581, Y. S. Lin, L. Ke, and C. Lee, are preparing a manuscript to be called "A split-ring-resonator-based polarization-insensitive broadband filter in terahertz frequency range."
34. F. Miyamaru, M. W. Takeda, and K. Taima, "Characterization of terahertz metamaterials fabricated on flexible plastic films: toward fabrication of bulk metamaterials in terahertz region," *Appl. Phys. Express* **2**(4), 042001 (2009).
35. F. Miyamaru, S. Kuboda, K. Taima, K. Takano, M. Hangyo, and M. W. Takeda, "Three-dimensional bulk metamaterials operating in the terahertz range," *Appl. Phys. Lett.* **96**(8), 081105 (2010).
36. D. B. Burckel, J. R. Wendt, G. A. Ten Eyck, A. R. Ellis, I. Brener, and M. B. Sinclair, "Fabrication of 3D Metamaterial Resonators Using Self-Aligned Membrane Projection Lithography," *Adv. Mater.* **22**(29), 3171–3175 (2010).
37. D. B. Burckel, J. R. Wendt, G. A. Ten Eyck, J. C. Ginn, A. R. Ellis, I. Brener, and M. B. Sinclair, "Micrometer-Scale Cubic Unit Cell 3D Metamaterial Layers," *Adv. Mater.* **22**(44), 5053–5057 (2010).

1. Introduction

Polymer devices have attracted tremendous research interest over the years due to their flexibility, stretchability, optical transparency and biocompatibility [1–3]. The ability to fabricate metal patterns on polymer substrates has realized many desirable applications, such as stretchable electronics [4], organic transistors [5] and flexible photolithography masks [6]. With the great progress in the research field of metamaterials [7–13] in the past decade, a lot of interesting optical applications have also come along. For example, the resonances can be actively tuned by stretching [14–17] the device or by wrapping it into different curvatures

[18]; perfect absorbers made on flexible substrates can be wrapped around curved surfaces and become effective in all directions [19]; such thin and flexible devices are also promising for stealth technology applications to hide from radar and other detections [20]. Among the commonly used polymer substrates in fabricating metamaterial devices, polydimethylsiloxane (PDMS) is one of the most favorable choices, for it enjoys a small Young's Modulus and low transmission loss [21], indicating great flexibility and stretchability as well as high transmission signal.

However, ways to pattern metals on PDMS surface have not progressed as fast in the past years. The PDMS metamaterials were mostly fabricated using direct deposition of metal followed by selective chemical etching [16,17,21]. Besides the possible contamination by wet chemicals, this process requires depositing an adhesion layer first to improve adhesion in the metal-PDMS interface. In fact, the low adhesion between PDMS and many metals has become an issue in other alternative fabrication methods as well, such as the metal transfer method. Due to its low surface energy, in metal transfer methods, PDMS is often used as the stamp where metal is first deposited onto and transferred to other substrates [5,22–24]. To reverse the process, an adhesion metal layer [22,25] or chemical promoter [26,27] to improve the adhesion in the metal-PDMS interface or/and a sacrificial layer [27] or release layer [22] to reduce the adhesion in the metal-stamp interface are required. On the other hand, these processes are often limited to fabricating only planar devices as the transferring takes place while the PDMS is cured and taking the shape of the stamp [26,27]. As curing of PDMS often takes about 2 to 3 hours in heated environment, such transfer techniques are often not suitable for fast production.

In this paper, we make use of the standard lift-off process to pattern metals on polyethylene terephthalate (PET) first, and then transfer them onto PDMS substrate with just oxygen plasma treatment. The transferring process is fast, convenient and free from wet chemicals. It takes place in room temperature with no requirement of adhesion or sacrificial layers. With such method, we show the realization of some unconventional metamaterial devices.

2. Experimental

In this work, 3M™ transparency film model PP2900 with surface roughness of about 20 nm [28] was used as the PET substrate, which was the host material where metal patterns were originally created on. It was first washed in acetone by sonication for 10 min and rinsed with deionized water. A layer of photoresist (Ultra-i 123) was then spin-coated on it at 800 rpm for 150 s, and soft-baked at 90°C for 90 s [3]. The micron-size patterns were defined using optical lithography while sub-micron dots and holes were patterned using Lloyd's Mirror interference lithography (LIL) system [28,29]. After exposure, the sample was developed in Microposit MF CD-26 developer for 1 min. Metals, aluminum (Al) and gold (Au) of 30 to 200 nm, were evaporated using Edwards FL 400 thermal evaporator. The process was completed by a lift-off step in acetone. The adhesion of the metal film to the PET substrate before the transfer process was confirmed by both a scotch tape test and sonication test. With no further treatment, metal films on the as-fabricated samples did not transfer to a sticky tape surface or come off during ultra-sound sonication.

The metal transfer process is illustrated in Fig. 1(a). The PET sample was first treated with oxygen plasma using a plasma enhanced chemical vapour deposition (PECVD) machine (SAMCO PD2400). The system had been modified to work as a regular RIE machine. The PET sample was placed on the cathode and was thus subject to both ion bombardment and chemical etching. A detailed study of the plasma etching mechanism and how the plasma condition relates to etching profile of the PET substrate has been done and reported previously [29]. It has been shown that as the power of oxygen plasma increases, more oxygen gets ionized in the chamber; the ions are more energetic and both lateral and vertical etch rate of the PET substrate increase. For this reason, the plasma power was set to be 200 W for efficient lateral etching to reduce the interfacial area where the metal pattern adhered to the PET surface, i.e. to create undercut to improve transfer yield. On the other hand, as the

PET substrate is insulating, the highly energetic ions that were accelerated by the electrical field in the sheath region towards the cathode got trapped into the PET surface and started to repel the metal layer. By bring a PDMS substrate into contact with the plasma treated PET sample, the metal was easily transferred due to van der Waals force. Through optimization experiments, we have set the plasma condition to be at 0.4 Torr, 200 W for 4 min. Combining lateral etching and charge trapping in one go, we successfully got rid of the sacrificial/ release layer that was often required to weaken the adhesion between the metal pattern and the carrier substrate [22,27,30], and lowered the adhesion between metal and PET so much that the van der Waals force was strong enough to lift the metal patterns and hold them in place on the PDMS surface. As a result, no pre-treatment of the PDMS surface is needed to enhance the metal adhesion, unlike many conventional methods to form metal patterns on PDMS surface—either by depositing metal directly on PDMS [16,17,21] or via metal transfer [22,25–27,30].

The PDMS used in this work was prepared using Dow Corning Sylgard 184 Silicone Elastomer Kit. The mixing ratio of the silicone elastomer and the curing agent was 10:1. Figure 1(b) and 1(c) show 80 nm-thick Al horseshoe patterns fabricated on PET and transferred to PDMS substrate afterwards, respectively. The linewidth, outer diameter, gap width and lattice constant of the pattern are 8, 30, 30 and 90 μm , respectively.

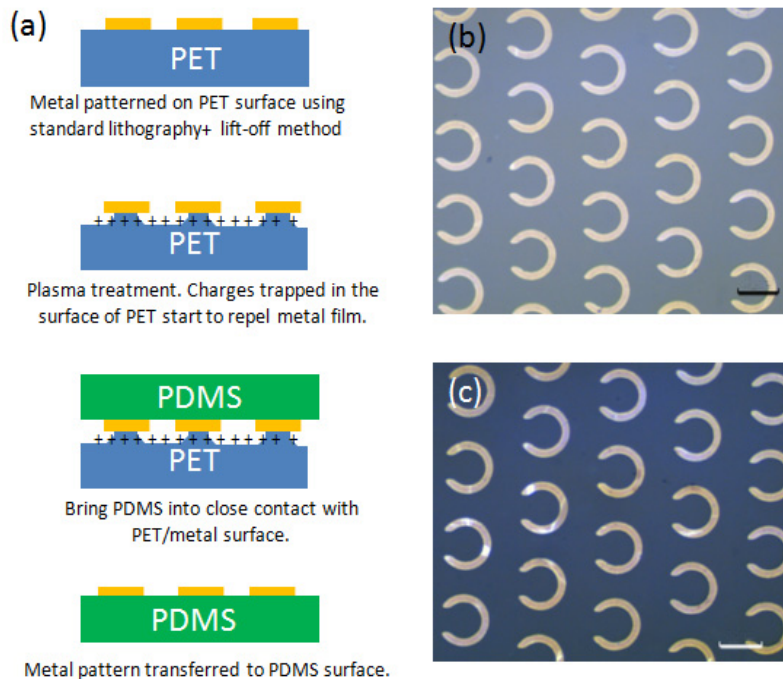


Fig. 1. (a) Process flow of the metal transfer method; (b) and (c) are microscopic images of an Al horseshoe pattern array patterned on PET and after transferred to PDMS. The scale bars in both images are 50 μm .

All electromagnetic (EM) responses of the devices in this work were characterized using terahertz time domain spectroscopy (THz-TDS, TeraView TPS 3000) in transmission mode with normally incident THz wave. The measured spectra were normalized to that of an unpatterned substrate of the same material and thickness. For devices fabricated on fabric and paper, the spectra were normalized to that of the same material with the same PDMS coating. Two incident polarizations were characterized for devices consisting SRR unit cells. When the polarization is parallel to the gap, it is referred to as 0° -polarization; when it is perpendicular across the gap, it is referred to as 90° -polarization.

3. Results and discussions

3.1 Fabrication of Au and Al patterns

Gold is known to assume different morphologies on PDMS, namely, microcracked, buckled, and smooth [31]. Such morphologies play an important role in affecting the electrical and optical properties of the gold film [31]. To investigate the morphologies of the gold patterns fabricated with our method, we fabricated large and small, discrete and continuous gold patterns on PET and transferred them onto PDMS substrates. The discrete patterns were split ring resonators (SRRs) [32] and nanodots, while the continuous patterns were the complementary split ring resonators (CSRRs) and film with nanoholes. The linewidth, side length, gap width and lattice constant of the SRRs were 12, 48, 12 and 100 μm respectively. The diameter of the nanodots and nanoholes were about 300 nm. The thickness of the SRRs, CSRRs, nanodots and film with nanoholes were 200, 200, 30 and 80 nm, respectively. The microscopic images of these transferred samples are shown in Fig. 2. The result demonstrates that such method is capable of transferring patterns with submicron feature sizes. On the other hand, however, we noticed that discrete gold patterns were generally smooth and crack free; microcracks were dominant in gold film with micron features; while both cracking and wrinkling were present in gold film with submicron features. The wrinkling and cracking can be attributed to the flexible yet brittle nature of the thin gold film. To complete the transferring process, the flexible PET substrate was peeled off from the PDMS substrate. A continuous film covering a large area was therefore transferred gradually from one end to the other, during which cracks and wrinkles were expected to appear. For metamaterial applications, such microcracks lead to changes in the capacitance of the device. As they are not induced in a controllable manner, the resulting changes are unpredictable and can vary the spectral response of the optical devices significantly and randomly. This implies that Au is not a suitable candidate when fabricating CSRR-based metamaterials using this method.

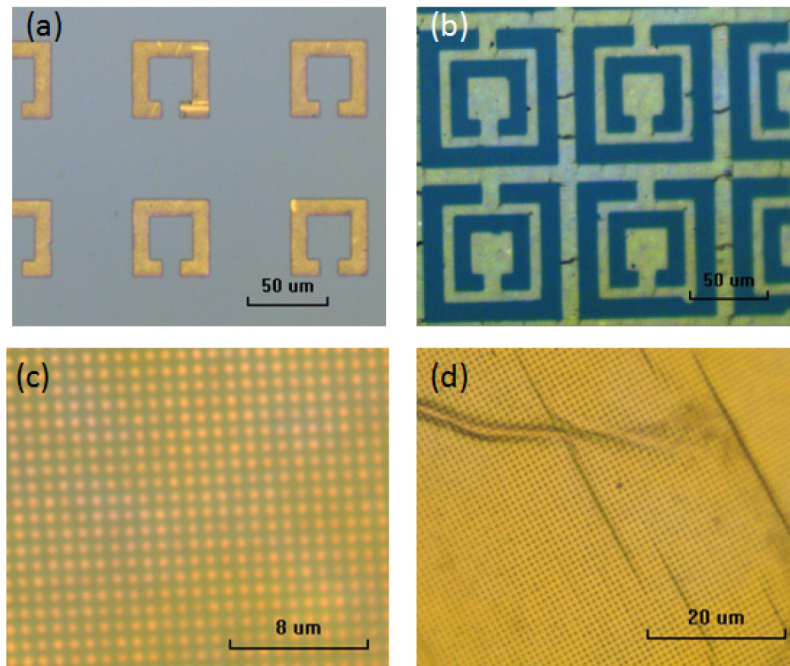


Fig. 2. Microscopic images of gold metal patterns transferred onto PDMS surfaces, namely, (a) discrete SRR pattern of 200 nm thick, (b) CSRR pattern of 200 nm thick, (c) nanodot array of 30 nm thick and (d) Au film with nanohole array of 80 nm thick.

The same processes were repeated using Al. All patterns were found to be smooth. As a comparison, the 80 nm-thick Al film with nanoholes on PDMS substrate is presented in Fig. 3. Non-cracking Al film covered an area of over 200 $\mu\text{m} \times 200 \mu\text{m}$ in average. An SEM image is also included in Fig. 3 for a close-up view of the quality of the transferred film. The difference between Au and Al is that aluminum oxide can be easily formed in oxygen plasma. Such a hard oxide layer holds the continuous film together and prevents wrinkles and cracks from growing.

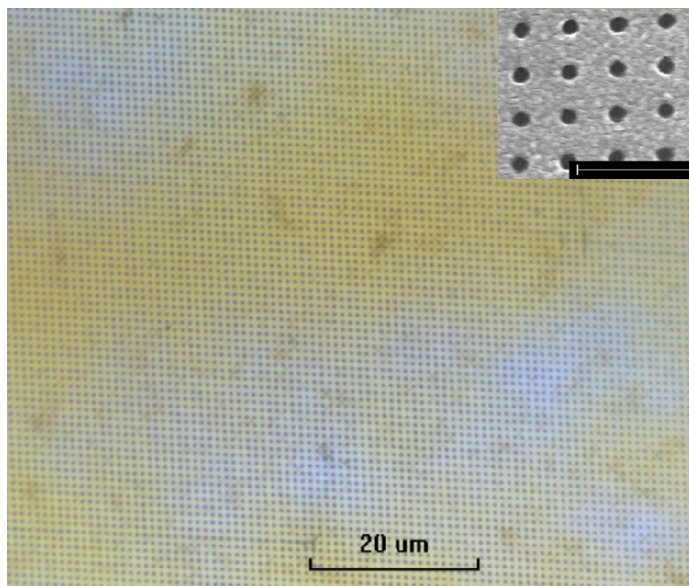


Fig. 3. Microscopic image of 80 nm-thick Al film with nanoholes transferred onto PDMS substrate with an inset of its SEM image. The scale bar in the inset is 2 μm .

Despite the different morphologies the metal patterns assume, the overall yields for transferring both Au and Al discrete and continuous patterns are estimated to be over 90%, by examining both the completeness of metal patterns on PDMS samples and remaining metal residue on respective PET samples after the transfer. Furthermore, to ensure sufficient undercut and charge trapping for high yield transfer, increasing plasma dose is beneficial when patterns with much larger line width are to be transferred.

3.2 Double-sided broadband THz filter

Two identical metamaterial devices were fabricated on PET substrates with unit cell of double split ring resonator as shown in Fig. 4(a). The outer and inner diameter, d_1 and d_2 , of the outer ring were 100 and 76 μm , respectively; d_1 and d_2 of the inner ring were 60 and 40 μm , respectively. The gap widths of both rings were 12 μm . The lattice constant was 114 μm . The 200 nm-thick metal patterns were then transferred onto the front and back side surface of a PDMS substrate of 500 μm thick, with the pattern on one side rotated 90° to the other, as shown in Fig. 4(b).

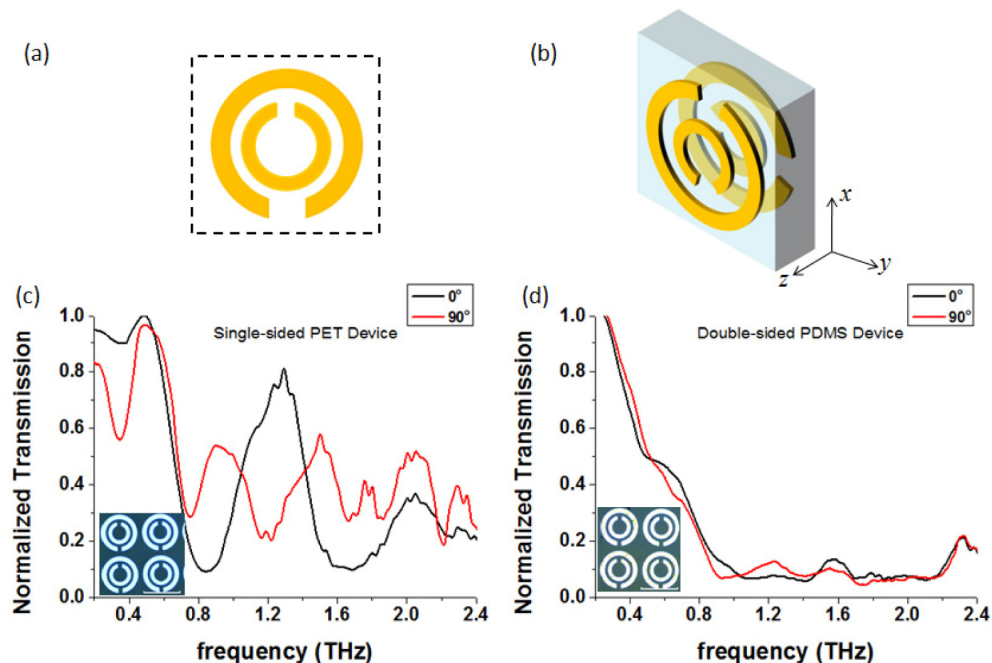


Fig. 4. (a) Illustration of the unit cell of the PET device; (b) illustration of the unit cell of the double-sided PDMS; and normalized transmission spectra of (c) single-sided PET device before transfer and (d) double-sided PDMS device after transfer with 0°- and 90°-polarized incidence. The insets in (c) and (d) are the microscopic images of both devices. The scale bars are both 100 μm .

According to the principles to be reported separately [33], the substrate thickness of the double-layered device is greater than the attenuation length of the resonant electromagnetic modes [34,35]; there is thus minimal coupling between the two layers of SRRs and they each resonate independently to the external EM field. In this way, without the need to align the unit cells, we are essentially cascading two narrowband THz filters with stopbands at alternating frequencies. When a light polarized in the x -direction transmits through the device in $-z$ direction, the front layer sees a 0°-polarized incidence, and filters out certain frequencies according to its narrowband filter characteristics. The partially filtered wave then excites the SRRs on the back layer as a 90°-polarized incidence and the resonant frequencies are filtered out again. For a y -polarized light, the principle works exactly in the same way except in a reverse order. In fact, for any randomly polarized light transmitting through the device, it can always be decomposed into x - and y -polarization, and gets filtered by the two filters sequentially. In other words, the transmission spectrum of the double-layered device equates to the superposition of those of the two individual narrow-band filters. As the narrow-band filters have no sharp band edges, superposition of their spectra merges their stopbands and exhibits a broad one.

In this way, the polarization-sensitive narrow-band filters on the PET are integrated into a polarization-insensitive broadband filter on the PDMS. The transmission spectrum of the PET device before transfer and the PDMS device after transfer were both characterized. The normalized transmission spectra are presented in Fig. 4(c) and 4(d). A flat stop band with transmission level around 10% is obvious in the spectrum of the PDMS device, which lasts from 0.9 THz to 2.3 THz. Noting the small size of the SRRs that support the resonances at THz range, the attenuation length of the resonant EM modes was estimated to be well below 100 μm [34]. Therefore, such a method poses little requirement on the substrate thickness as many freestanding substrates are above this thickness and can act as the dielectric layer separating two independent layers of SRRs. Also, as the reflection of the PDMS surface is

relatively low, the Fabry–Pérot resonance is much weaker as compared to the EM resonances; it is almost indistinguishable in the measured spectra.

The fact that broadband filters can be easily obtained from conventional narrowband devices can greatly speed up research in the relevant field, and extend their applications further.

3.3 Metamaterial devices on unconventional substrates

With PDMS as the medium, many unconventional substrates can now be used in metamaterial fabrication. Here, we used only Al SRR patterns as a demonstration. The dimensions are the same with the SRRs shown in Fig. 2(a). The patterns were fabricated on a piece of fabric cut from a cotton t-shirt, a piece of cleanroom tissue paper and a tree leaf. A very thin layer of uncured PDMS was applied on to the surfaces of these materials using a cotton swab. The samples were then cured on a hotplate at 70°C for 10 min. The cured PDMS layer covering the surfaces measures about 20 μm thick. Metal patterns pre-fabricated on PET substrates were then transferred onto the PDMS-covered substrate surface in the same way as described in Section 2. The optical and microscopic images of such devices are presented in Fig. 5(a) to 5(d). The metamaterial patterns on all three kinds of substrates showed no significant difference in appearance. All patterns were uniformly transferred and preserved the orderly array as they were fabricated on PET.

For comparison purpose, we also transferred the metal pattern on to a flat PDMS substrate of 500 μm thick. The transmission spectra of the devices on PET, fabric, paper, leaf and PDMS substrates were then characterized with 90° incident polarization. Due to the great absorptive nature of tree leaf in the THz range, very low level of transmitted signals were detected from both patterned and un-patterned tree leaf substrates. The normalized spectra for the other devices are presented in Fig. 5(e). It is interesting to note that while PET device has a transmission dip at 0.82 THz, all other devices on PDMS substrate or PDMS-mediated substrates resonate at about the same frequency, 0.89 THz. This is important in designing metamaterial devices on unconventional substrates, as the resonant frequency can be calculated by assuming the substrate as pure PDMS.

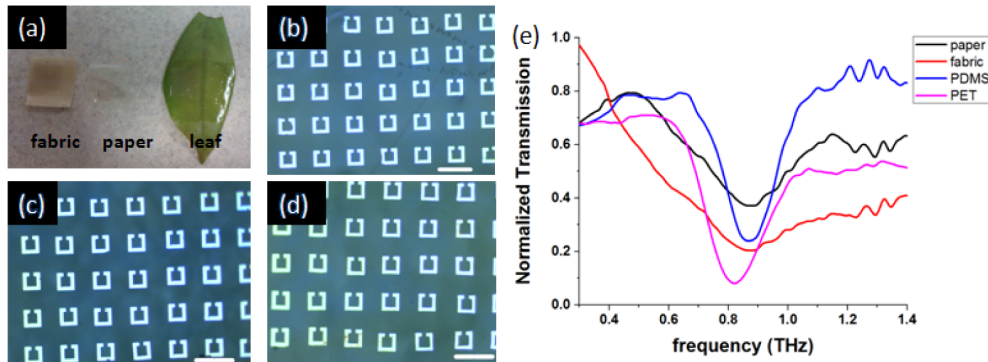


Fig. 5. (a) Metamaterial patterns transferred onto various substrates including fabric, paper and a leaf. (b) to (d) are microscopic images of the patterns on fabric, paper and leaf, respectively. (e) presents the spectra of devices on paper and fabric as well as that of a PET substrate (before transfer) and a PDMS substrate (after transfer). All devices in (e) have the same metal pattern. The scale bars in (b) to (d) are all 100 μm .

3.4 Non-planar metamaterial devices

Previous endeavors in fabricating 3D metamaterials have resorted to complicated lithography and metallization processes, such as Membrane Projection Lithography (MPL) which combines patterning membrane over a cavity and serial directional evaporation [36,37]. The metal transfer method proposed here can simplify such processes as it allows easy

metallization on non-planar surface. For example, to transfer metal patterns onto the curved surface of a PDMS cylinder can be simply accomplished by rolling the cylinder on a plasma-treated PET sample with the desired metal patterns on it. We have exploited this method to fabricate SRR patterns with dimensions same as those shown in Fig. 2(a) on PDMS cones, cylinders and cubes, as shown in Fig. 6(a). The metal patterns transferred are uniform and intact. A representative image of that on PDMS cylinder is shown in Fig. 6(b). These results will pave the way towards 3D isotropic metamaterial devices.

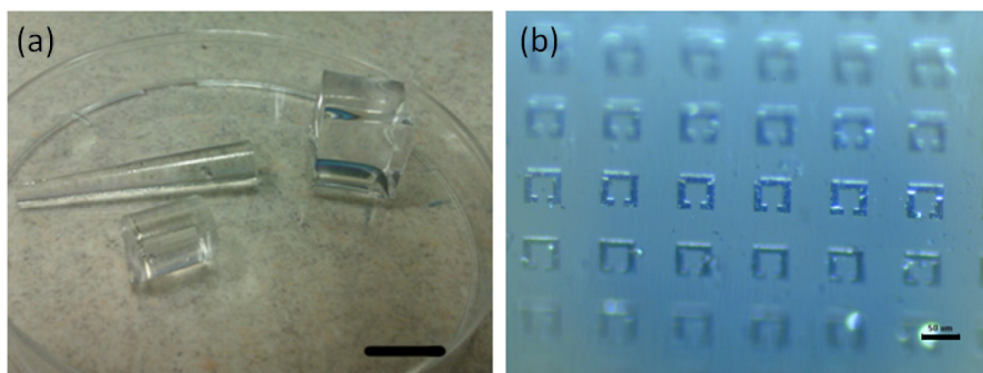


Fig. 6. (a) Optical image of non-planar metamaterial devices with metal patterns fabricated on a PDMS cone, a cylinder and a cube; and (b) microscopic image of the cylindrical metamaterial. The scale bars in (a) and (b) are 1 cm and 50 μm , respectively.

4. Conclusion

We have introduced a straightforward metal transfer method to create metal patterns on PDMS surface. With this, no adhesion layer or sacrificial layer is required. The transferring process is fast and wet chemical free, and its resolution can go to sub micron scale. We looked into the morphologies of the transferred Al and Au patterns and found that Al patterns are generally free from microcracks and wrinkles whereas Au patterns are only smooth when they are discrete. Using this method, some unconventional metamaterial devices are fabricated and characterized, including double-sided broadband filter, devices on PDMS-mediated everyday material surfaces and non-planar surfaces. Such results will expedite the research in metamaterials as they not only simplify the fabrication process, but also bring about devices that have not been easily realized before.

Acknowledgments

The authors acknowledge the financial support from research grant of MOE AcRF Tier 2 - MOE2012-T2-2-154 under WBS No. R-263-000-A59-112 at the National University of Singapore.